J. Fluid Mech. (1996), *vol.* 315, *pp.* 31–49

An experimental study of the influence of riblets on transition

By G. R. GREK, V. V. KOZLOV AND S. V. TITARENKO
Institute of Theoretical and Applied Mechanics, Russian Academy of Sciences, Siberian Branch, 630090 Novosibirsk, Russia

(Received 30 May 1994 and in revised form 11 December 1995)

An experimental study of the effect of riblets on three-dimensional nonlinear structures, the so-called Λ-vortices on laminar–turbulent transition showed that riblets delay the transformation of the Λ-vortices into turbulent spots and shift the point of transition downstream. This result is opposite to the negative influence of such ribbed surfaces on two-dimensional linear Tollmien–Schlichting waves (the linear stage of transition). Thus, the ribbed surface influences laminar–turbulent transition structures differently: a negative influence on the linear-stage transition structures and a positive influence on the nonlinear-stage transition structures. It is demonstrated that transition control by means of riblets requires special attention to be paid to the choice of their location, taking into account the stage of transition.

1. Introduction

So far, many studies connected with riblets have been carried out in the turbulent boundary layer, where riblets have a favourable influence on drag reduction. Some of the earliest and more important results were obtained by Walsh (1979; 1983) and Walsh & Linderman (1984). They showed that drag reduction could be obtained when the height of the riblet structure expressed in wall units, $s^+ = su^*/\nu$, is below 30; the maximum of 7–8 % reduction occurred when s^+ is about 15. Here s is the height and base of the riblets, u^* is the friction velocity of the turbulent boundary layer and ν is the kinematic viscosity. They also found that triangular grooves are among the most effective in reducing drag. Investigations of carefully optimized riblet models in the work by Coustols & Coustex (1989) showed that maximum gains of skin-friction reduction occurred for triangular-groove models such that h^+ (rib height scaled with the inner variable of the turbulent boundary layer) was less than 18 and this result was close to the same parameter obtained by Walsh & Linderman (1984). A good review of some recent developments concerning drag reduction by passive devices is given in Savill (1989). However, the physical mechanism of this influence has not yet been found and the role of the riblets in this process remains unclear. One possible concept is that drag reduction is due to the changes in the near-wall coherent structures, as presented, in particular, by Bacher & Smith (1985), Bechert, Bartenwerfer & Hoppe (1989) and Choi (1989). These works demonstrated the importance of the impeding of the cross-flow by longitudinal ribs in drag reduction. The coherent structures in the turbulent boundary layer are similar to the vortex structures of transition and an experimental study in a laminar boundary layer by Smith *et al.* (1989) showed that this similarity is very promising for understanding the mechanism by which riblets influence the coherent structures of the turbulent boundary layer.

Studies of the influence of riblets on laminar–turbulent transition have been presented in only a few papers and the conclusions of these works are sufficiently contradictory for a more detailed investigation to be required. Hot-wire anemometry studies by Djenidi, Anselmet & Fulachier (1987) of large riblets in water have suggested drag reduction of up to 4% even in laminar flow over riblet. No favourable influence of riblets on laminar–turbulent transition could be found by Belov, Enutin & Litvinov (1990), whether the riblets were located along or across the flow. It should be noted that in this case riblets were placed on the entire surface of the flat plate where the transition takes place. The work by Kozlov *et al.* (1990) demonstrated that longitudinal grooves on a test-plate surface result in either a positive or negative influence on bypass transition under the influence of high free-stream turbulence ($\epsilon = 1.5$–3%), depending on the pressure gradient and leading-edge shape of their test plate. In experimental investigations carried out by Neumann & Dinkelacker (1991) it was found that riblets delay the development of initial turbulent structures in the transitional zone of the flow on a body of revolution. Numerical simulation by Chu, Henderson & Karniadakis (1992) showed that, in comparison with a smooth surface, in the transitional regime there is drag reduction with riblets. The basic conclusions of a calculation by Luchini (1993) are that grooving has a destabilizing effect upon Tollmien–Schlichting instability but a stabilizing one on Taylor–Görtler instability.

The contradictory nature of these studies seems to be connected with looking at the riblets influence on the disturbances without distinguishing these disturbances in terms of their types and stages of development because of the difficulty in obtaining detailed information about the characteristics of the development of the different disturbances leading to so-called 'natural' laminar–turbulent transition. Thus the main purpose of this paper is to study the influence of riblets on Tollmien–Schlichting (TS) wave development at linear (i.e. two-dimensional TS waves) and nonlinear (i.e. Λ-structures)) stages of transition. These disturbances were excited in a laminar boundary layer in a controlled manner. This method gave the possibility of obtaining new information about the influence of riblets on the different disturbances involved in transition and a deeper understanding of the nature and mechanism of this influence, with aim of a possible explanation of, or at least a first step towards, the effect of riblets both on transition and on the drag reduction mechanism in a turbulent boundary layer.

2. Experimental set-up and measurement technique

The experiments were performed in a low-turbulence wind tunnel (T-324) at the Institute of Theoretical and Applied Mechanics of the Siberian Branch of the Russian Academy of Sciences (Novosibirsk). It is closed return wind tunnel with a 4 m long test section and 1×1 m cross-section, preceded by a contraction with ratio 17:1. The streamwise velocity fluctuation is less than 0.04% at the velocity of 8.2 m s^{-1} for the present experiment.

The flat plate (1) in figures 1 and 2, of 1.5 m length, 1 m width and 10 mm thickness, was mounted vertically in the working section of the wind tunnel. All measurements were carried out at a free-stream velocity 8.2 m s^{-1} and free-stream turbulence of less than 0.04%. The flat-plate leading edge was composed of two conjugate semiellipses of axes of 2:132 mm on the working side of the plate and of 8:132 mm on the opposite side. The model is carefully installed in order to obtain a zero streamwise pressure gradient, which was uniform within the area of measurements.

A 15 mm thick steel disk, of 160 mm diameter (see figure 1), and a 1.2 mm thick plastic plate, 285 mm long, 285 mm wide (see figure 2) were utilized as riblet plates, designated 1 and 2 respectively. All riblets have a symmetrical triangular shape with

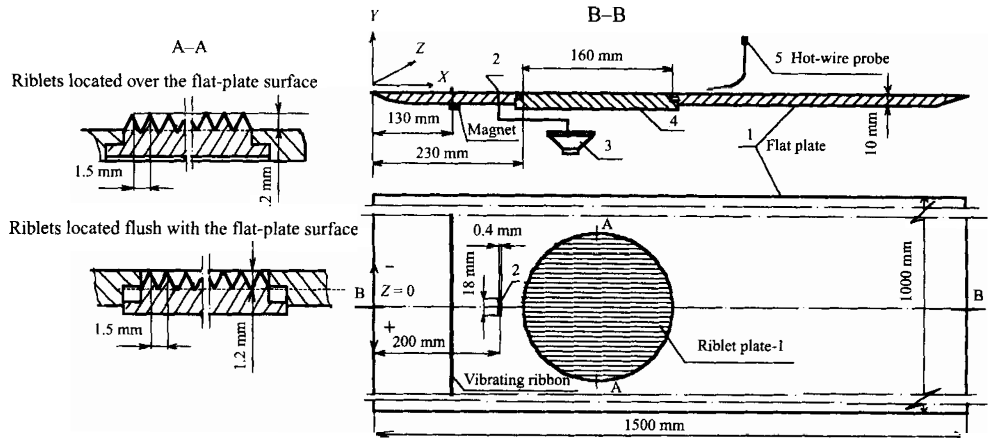

FIGURE 1. Experimental set-up 1.

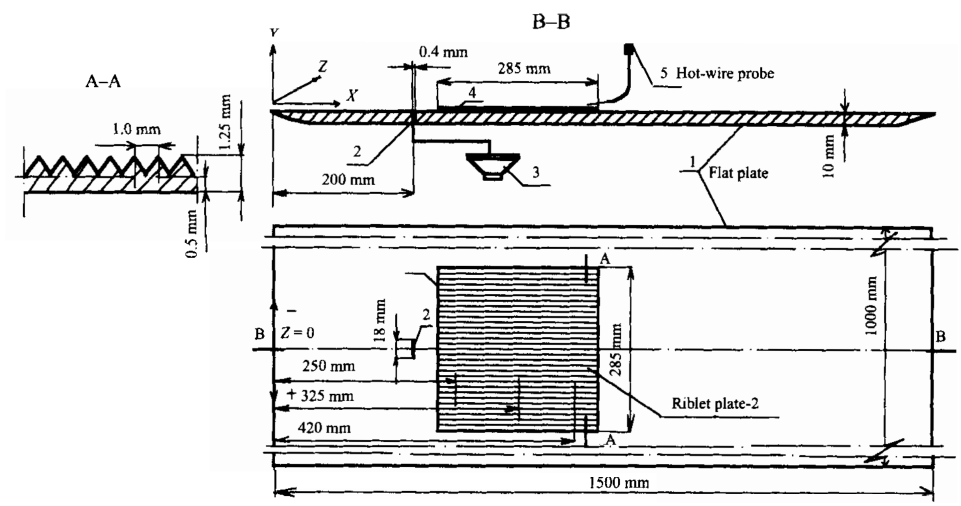

FIGURE 2. Experimental set-up 2.

sharp edges. The shape, height (h) and lateral spacing (s) of the riblets are shown in figures 1 and 2 (see cross-sections A–A); $h_1 = 1.2$ mm, $s_1 = 1.5$ mm for riblet plate 1 and $h_2 = 0.75$ mm, $s_2 = 1.0$ mm for riblet plate 2. Riblet plate 1 can be located with the riblet peaks either flush with or above the flat-plate surface and with the riblets along or across the flow. Riblet plate 2 could be located only above the flat plate surface and with along-flow riblets. A symmetrical triangular shape for the riblets was chosen because more often than not this is used for drag reduction and moreover this shape is simpler to manufacture. The riblet height and spacing were optimized using preliminary investigations by Grek, Kozlov & Titarenko (1993) concerning the influence of these dimensions on Λ-vortex development. The height and spacing were varied from 0.3 to 3 mm and from 0.5 to 3 mm) respectively but a favourable riblet influence on Λ-vortex behaviour was found only for heights ranging from 0.7 to 1.2 mm and for spacing ranging from 1.0 to 1.5 mm. About 30 spectral amplitudes for each experimental position (i.e. at $X = 420$ mm, $Y = Y(u'_{max})$ but for different states of the flat-plate surface), obtained by analysis of single oscilloscope traces measured in the plane of symmetry of Λ-vortices propagating on the smooth and riblet surfaces, were ensemble-averaged and from this information the optimum riblet sizes were determined.

Periodic two-dimensional waves were excited by a vibrating ribbon positioned 130 mm downstream from the leading edge. The ribbon was placed in the magnetic field of a permanent magnet mounted in a hollow on the reverse side of the plate, and it was vibrated by feeding it with an electric current of the desired amplitude and frequency (the ribbon is operated at 102 Hz in the present case).

Three-dimensional localized disturbances were introduced into the boundary layer by means of a dynamic loudspeaker (3) through narrow slit (2) located at a distance of 200 mm from leading edge of the flat plate (see figures 1 and 2). The loudspeaker was connected to a generator of square pulses of frequency about 0.5 Hz. On the other hand, three-dimensional nonlinear wave packets of the K-regime of boundary layer transition (see Saric 1994) were created by vibrating the ribbon at higher amplitudes.

A hot-wire anemometer of constant temperature was used for measurements of the longitudinal components of the mean velocity ($\bar{u}$) and the fluctuations of the flow velocity (u') in accordance with the coordinates shown in figures 1 and 2 where X, Y, Z denote the streamwise, normal to the wall and the spanwise directions, respectively. Note, that r.m.s.-values, u'_f, of the velocity fluctuations are measured for the narrow frequency band ($\Delta f = 4$ Hz) of the fundamental TS wave frequency ($F = 102$ Hz). On the other hand, the fluctuations of flow velocity (u') for the Λ-vortices is measured from the amplitude of a single oscilloscope trace signal (see figures 9(*a*) and 15) or the time-averaged (3 min) maximum amplitudes of the signals taken as 'peak-to-peak' (see figure 10) or ensemble-averaged (20 single realizations) signals as presented in figures 9(*b*), 12, 13 and 14. The u'_{max} value is the maximum amplitude of an ensemble-averaged signal (see figure 11).

The probe calibration, data acquisition and data reduction were conducted by means of a MacADIOS-ADIO analog-to-digital converter (GW instruments) connected to a personal computer Macintosh Classic II. In order to obtain a synchronized hot-wire signal, the Tollmien–Schlichting waves and the localized vortex disturbances appearing in the laminar boundary layer were synchronized by means of signals generated by disturbances sources.

3. Results of the measurements and discussion

As stated above, the triangular riblets height and lateral spacing were chosen from a preliminary experiment, where a positive riblet influence on Λ-vortex development was found for the height $1.2 \geqslant h \geqslant 0.75$ mm) and lateral spacing $1.0 \geqslant s \geqslant 1.5$ mm. The present investigation includes measurements of boundary layer flow disturbed by artificial TS waves and localized three-dimensional disturbances, Λ-vortices. In the first case, riblet plate 1 was used, where the ribs were located flush with the flat-plate surface or above it and with riblets along or across the flow (the lateral distance (spacing) between the ridges is $s_1 = 1.5$ mm and their height is $h_1 = 1.2$ mm). In the second case, we used riblet plate 1 placed only above the flat-plate surface and with the riblets along or across the flow and riblet plate 2 placed above the flat-plate surface with the ribs located only along the flow (the lateral distance (spacing) between the ridges is $s_2 = 1.0$ mm and their height is $h_2 = 0.75$ mm). Measurements of the TS wave behaviour were carried out at the flat-plate centreline ($Z = 0$), at different values of Y, and from $X = 200$ mm to $X = 407$ mm downstream, corresponding to Reynolds numbers ($Re_X = U_\infty X/\nu$) between 1.09×10^5 and 2.22×10^5, while the measurements of Λ-vortices behaviour were carried out at the five different distances downstream

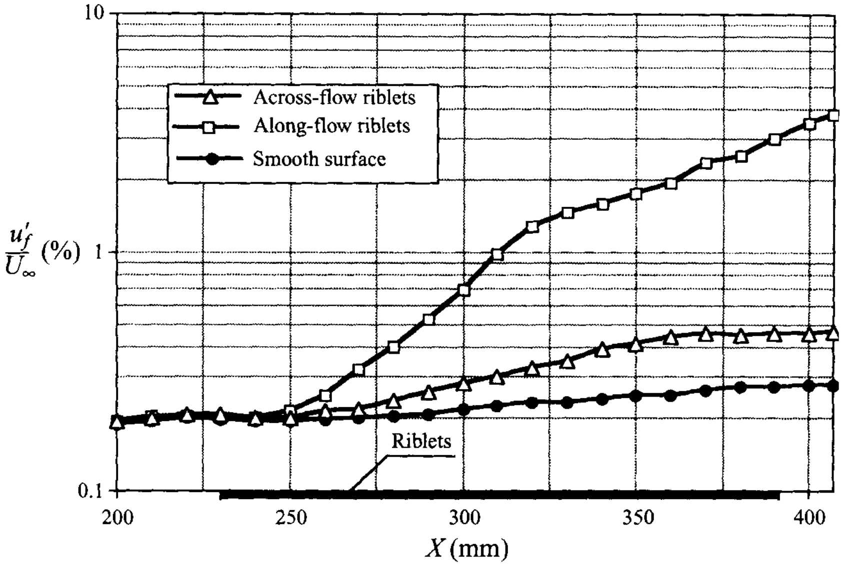

FIGURE 3. Amplification curves of the Tollmien–Schlichting waves developing on the flat-plate surface and on riblet plate 1 located flush with the flat-plate surface, $Z = 0$, $Y = Y(u'_{f\,max})$.

X (mm)	δ (mm)	δ^* (mm)	$U_\infty \delta^*/\nu$	$(U_\infty X/\nu) \times 10^{-5}$
200	3.0	1.03	563	1.09
235	3.3	1.13	618	1.28
290	3.64	1.25	683	1.58
300	3.7	1.27	694	1.64
320	3.82	1.32	722	1.75
335	3.9	1.34	732	1.83
370	4.1	1.4	765	2.02
407	4.3	1.48	809	2.22
420	4.38	1.5	820	2.29
430	4.43	1.52	831	2.35
450	4.54	1.56	853	2.46

TABLE 1. Experimental parameters

($X = 320, 335, 370, 420, 430$ mm) for the Reynolds number range from $Re_X = 1.75 \times 10^5$ to $Re_X = 2.35 \times 10^5$ and at different spanwise (Z) and normal to the surface (Y) distances. Overall characteristics of the undisturbed flow at the main stations for which results are presented here are listed in table 1. Note that the undisturbed flow in the boundary layer without riblets had mean velocity profiles close to the Blasius profile for all the ranges of measurements.

The riblet lateral spacing was normalized by 'outer' (δ^*) and 'inner' (ν and u^*) variables. Non-dimensional lateral spacing is $s^+ = su^*/\nu$, where $u^* = (\nu\,|\partial u/\partial y|_{y=0})^{1/2}$ is the laminar friction velocity and $|\partial u/\partial y|_{y=0} = 0.332 U_\infty/\delta$ is the mean velocity gradient on the wall, where $\delta \sim (\nu X/U_\infty)^{1/2}$. In the range of Re_X considered, the non-dimensional lateral spacings normalized by inner variables are $26 \geqslant s_1^+ \geqslant 21$ ($17 \geqslant s_2^+ \geqslant 14$) and normalized by outer variable (s/δ^*) are $1.4 \geqslant (s/\delta^*)_1 \geqslant 1.0$ ($0.9 \geqslant (s/\delta^*)_2 \geqslant 0.6$) for riblet plates 1 and 2, respectively.

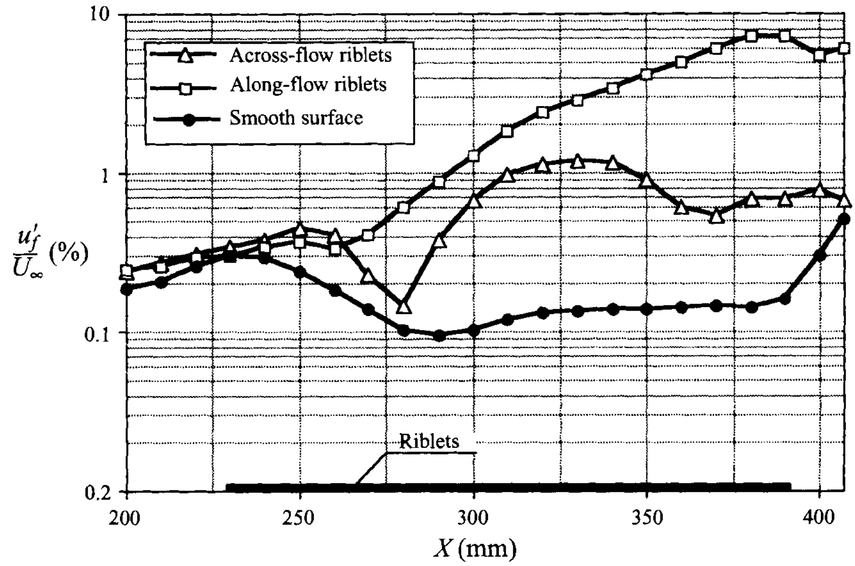

FIGURE 4. Amplification curves of the Tollmien–Schlichting waves developing on the flat-plate surface and on riblet plate 1 located above the flat-plate surface, $Z = 0$, $Y = Y(u'_{fmax})$.

3.1. *Effects on the linear development of forced Tollmien–Schlichting waves*

Riblet plate 1 ($s^+ = 22$–26) was used in this experiment.

3.1.1. *Amplification curves*

Amplification curves of the Tollmien–Schlichting (TS) waves that developed at the smooth and ribbed surfaces of the flat plate, when the riblet plate was located flush with the flat-plate surface and the riblets were placed along or across the flow are shown in figure 3. The smooth surface was created by replacing the riblet plate by a smooth plate. The disturbance amplitude is given in a logarithmic scale as a percentage of the free-stream velocity.

It is seen from figure 3 that locating the riblets along the flow leads to considerable amplification of the TS waves in comparison with their development on the smooth surface, and that locating the riblets across the flow leads to small amplification of the TS waves in comparison with their development on the smooth surface.

Amplification curves of the TS waves that developed on the smooth and ribbed surfaces of the flat plate, when the riblet place was located above the flat-plate surface and riblets placed along or across the flow are shown in figure 4. The tops of the riblets protruded 1.2 mm into the flow above the flat-plate surface and the bottoms of riblet valleys were at the same height as the surface of the flat plate.

Figure 4 shows that the general picture of the riblet influence on the TS wave development remains the same as in figure 3: the amplification of the TS waves for riblets located along the flow is much higher than across the flow or on the smooth surface, and cross-flow riblets disturb the boundary layer less than along-flow riblets. However, in spite of similarity of the general picture of TS wave growth presented by figures 3 and 4, specific inflexions of the amplification curves in the region near the steps between the plate and the beginning and end of the riblet surface are seen for all three curves in figure 4. In order to define the cause of this phenomenon the mean velocity profiles were measured over a smooth plate installed both flush with and above

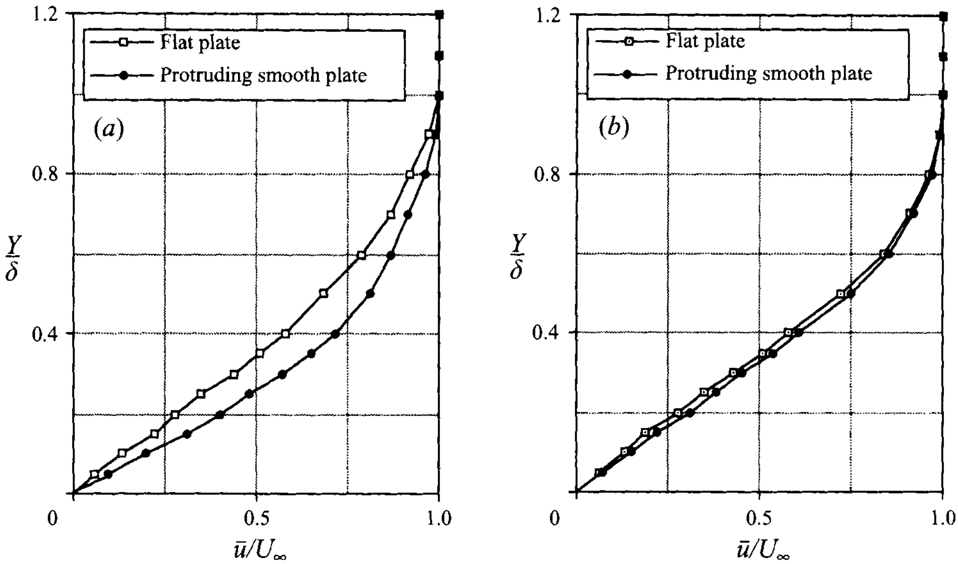

FIGURE 5. Mean velocity profiles ($\bar{u} = f(Y)$) measured both on the flat-plate surface and on a protruding smooth plate, $Z = 0$. (*a*) $X = 235$ mm, (*b*) $X = 290$ mm.

the flat-plate surface in the region of the first step and near the plate centre. The results of these measurements are presented in figure 5, and described in §3.1.2.

3.1.2. *Mean flow*

Two profiles of the mean velocity measured for the smooth plate located above and flush with the flat-plate surface are shown in figure 5 at $X = 235$ mm beyond the step, and at $X = 290$ mm, near the plate centre. The smooth-plate protrusion into the flow is 1.2 mm, corresponding to the height of the riblet tips when the riblet plate is installed above the flat-plate surface. It is seen that the mean velocity profile measured at $X =$ 235 mm is more rounded and, in correspondence with non-viscous instability theory, is more stable than the same profile measured on the smooth flat-plate surface at $X =$ 235 mm. Apparently, the changes in the amplification curve behaviour observed in figure 4 at step regions in comparison with their behaviour shown in figure 3 are connected with mean flow changes. This fact was noted by Boiko *et al.* (1990), where two-dimensional TS wave development on a step was studied and similar behaviour of the amplification curves found.

Measurements carried out far downstream from the step at $X = 290$ mm (near the centre of the smooth plate) presented in figure 5(*b*) show that the mean velocity profile measured on the protruding smooth plate becomes similar to that measured on the smooth flat plate and the behaviour of the amplification curves presented in figure 4 becomes the same as in figure 3, while they differ again near the second step at $X =$ 390 mm (not shown).

The mean velocity profiles measured on riblet plate 1 located flush with the flat-plate surface and above the flat-plate surface for riblets placed along or across the flow at $X = 300$ mm are shown in figure 6. It is seen from the plots that mean velocity profiles measured on the riblets located along and across the flow are the same, except in a narrow region inside the riblet valleys when the riblet plate is placed above the flat-plate surface. This region was not investigated because the probe sensitive element size

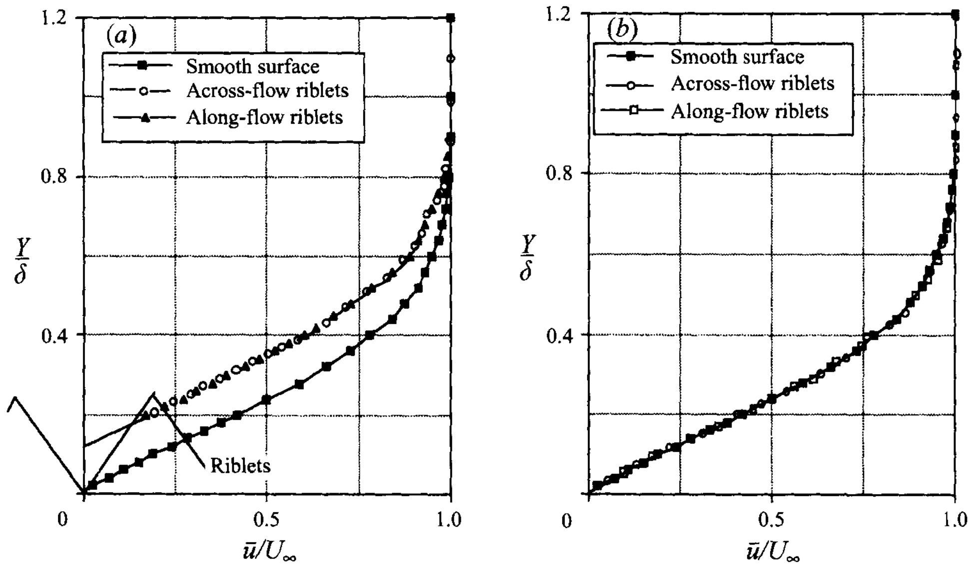

FIGURE 6. Mean velocity profiles ($\bar{u} = f(Y)$) measured on the flat-plate surface and on the riblet plate at $X = 300$ mm, $Z = 0$. (*a*) Riblets above the flat-plate surface, (*b*) riblets flush with the flat-plate surface.

(1 mm) was too large. The mean velocity profiles measured on the riblets located above the flat-plate surface have shifted up by about half the height of the riblets from profiles measured at the smooth surface. Shifting the mean velocity profiles corresponding to riblet measurements down by half height of ribs, it was found that all profiles collapse quite well onto a single curve. Thus, the profiles measured at smooth and riblet surfaces on the flat plate remain unchanged for the bulk of the flow field and an explanation for the different amplification rates of the TS waves at the smooth flat-plate surface and at riblets located along and across the flow cannot to be made using these results. Probably, it is therefore not connected with the mean flow characteristics.

Note that measurements of the mean velocity profiles are presented only over the riblet valleys (see figure 6) where the riblet origin is $0.5h$ but, on the other hand, the riblet origin for the same measurements obtained in the work by Grek *et al.* (1993) over the riblet peak is approximately $1.0h$. Thus, the virtual origin position of the mean velocity profiles is changed depending on whether the flow is above riblet peaks or valleys.

3.1.3. *Fluctuations of flow velocity*

The fluctuations of flow velocity profiles of TS wave development measured on riblet plate 1 located flush with and above the flat-plate surface for riblets were placed along or across the flow at $X = 300$ mm are shown in figure 7. The profiles on the riblets located along or across the flow for the riblet plate placed flush with the flat-plate surface and on the smooth flat plate are very similar but measurements on the riblet plate located above the flat-plate surface are different for the riblets located along and across the flow. Apparently, this is connected with the nonlinear stage of TS wave development for riblets located along the flow, where the amplitude of disturbances attains a level of 10%. Also, in the flush-mounted case, where differences of the mean velocity and velocity fluctuations profiles on the riblets placed along and across the flow were not observed, the amplification rates of the TS waves for the riblets located

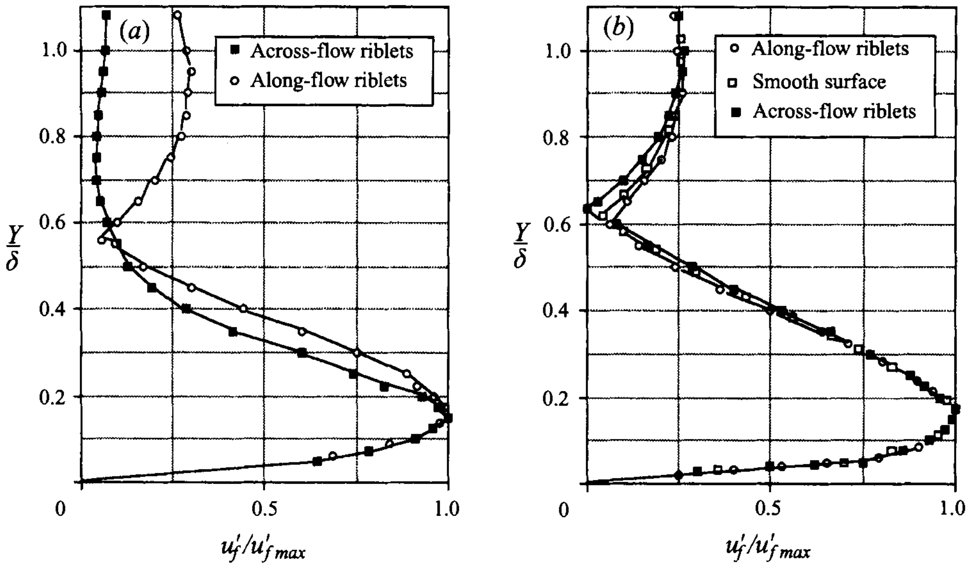

FIGURE 7. Fluctuations of flow velocity profiles ($u'_f = f(Y)$) of Tollmien–Schlichting waves measured on the flat-plate surface and on the riblet plate at X = 300 mm, Z = 0. (*a*) Riblets above the flat-plate surface, (*b*) riblets flush with the flat-plate surface.

along the flow is much higher than for across-flow riblets (see figure 3). A possible explanation of this phenomenon is connected with the presumption that two-dimensional TS waves were less disturbed by riblets located across the flow than by riblets located along the flow because the former were parallel to the plane wave front, while in the latter case the riblets were across the plane wave front and TS waves underwent a three-dimensional distortion on the riblet ridges. A greater transition acceleration on riblets located along the flow than across the flow was noted in Belov *et al.* (1990), where the riblets were placed in region of the two-dimensional TS wave growth.

Note that the riblets' influence on the two-dimensional TS waves was investigated only after the study of the effects of these riblets on the nonlinear Λ-vortices because it was interesting to consider their influence on disturbances at the linear stage of transition. Results of those studies nonlinear are opposite to the present riblets' influence on the three-dimensional transition structures but this negative riblet effect on the disturbances at an initial stage of transition is also in good agreement with the numerical simulation by Chu *et al.* (1992) and the asymptotic analysis by Luchini (1993). On the other hand, observations by Dinkelacker, Nitsche-Kowsky & Reif (1987) showed that some sharks have smooth scales close to the stagnation lines where the flow can be expected to be laminar or transitional and ribbed scales elsewhere. This is also in excellent agreement with the present findings.

3.2. *Effect on the development of* Λ*-vortices on ribbed surfaces*

A visualization of the transformation of a single nonlinear wave packet (the so-called Λ-vortex) into a turbulent spot is shown in figure 8(*a*). The Λ-vortex is an element of the three-dimensional distortion of a two-dimensional TS wave at the nonlinear stage of its development; it is shown in Grek, Kozlov & Ramasanov (1989). We studied the riblet influence on the development of this Λ-vortex and riblets were mounted at various stages of its development.

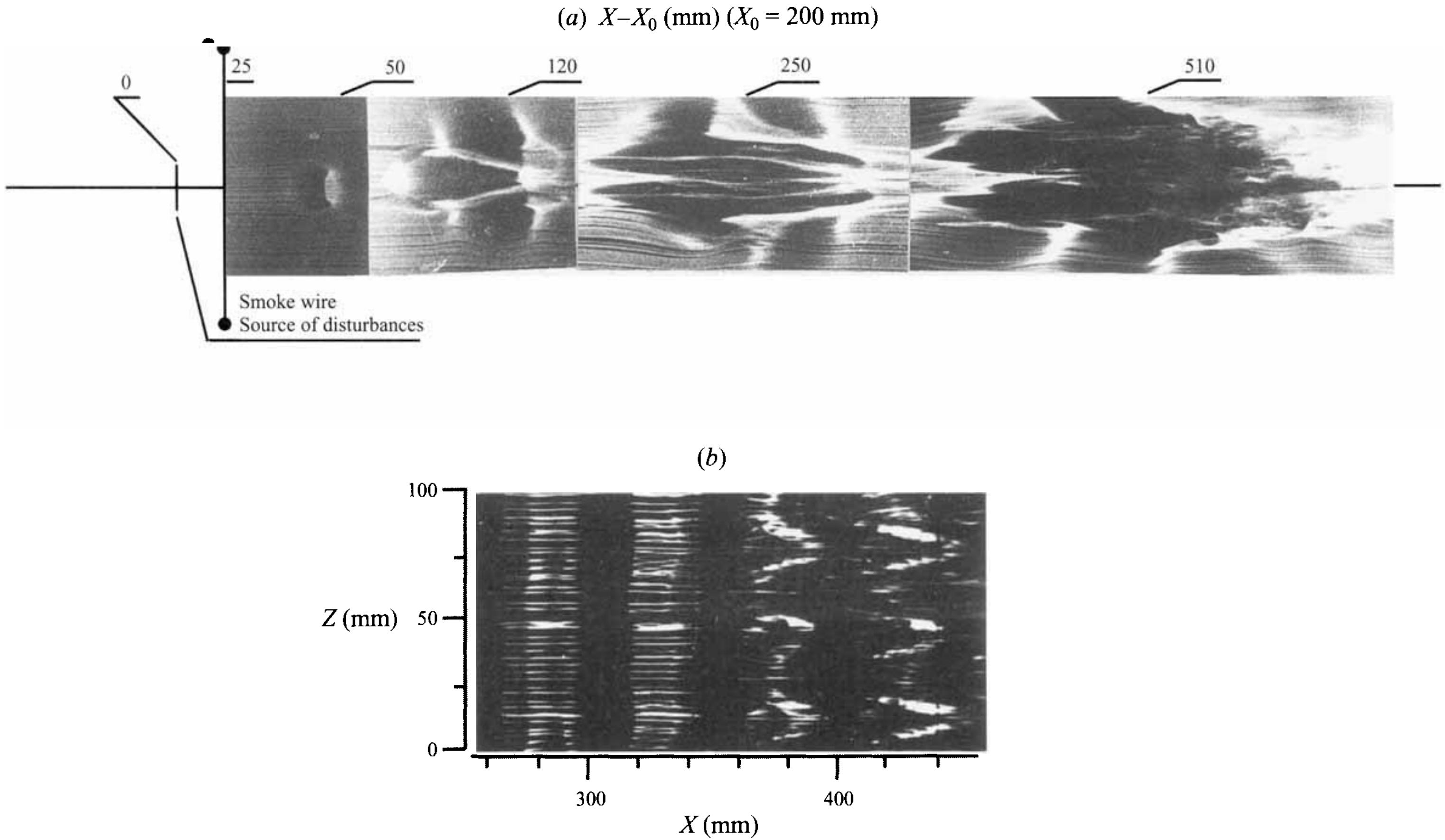

FIGURE 8. Visualization of (*a*) the transformation of a single nonlinear wave packet (Λ-vortex) into a turbulent spot, (*b*) the formation of a group of Λ-vortices in the K-regime of transition.

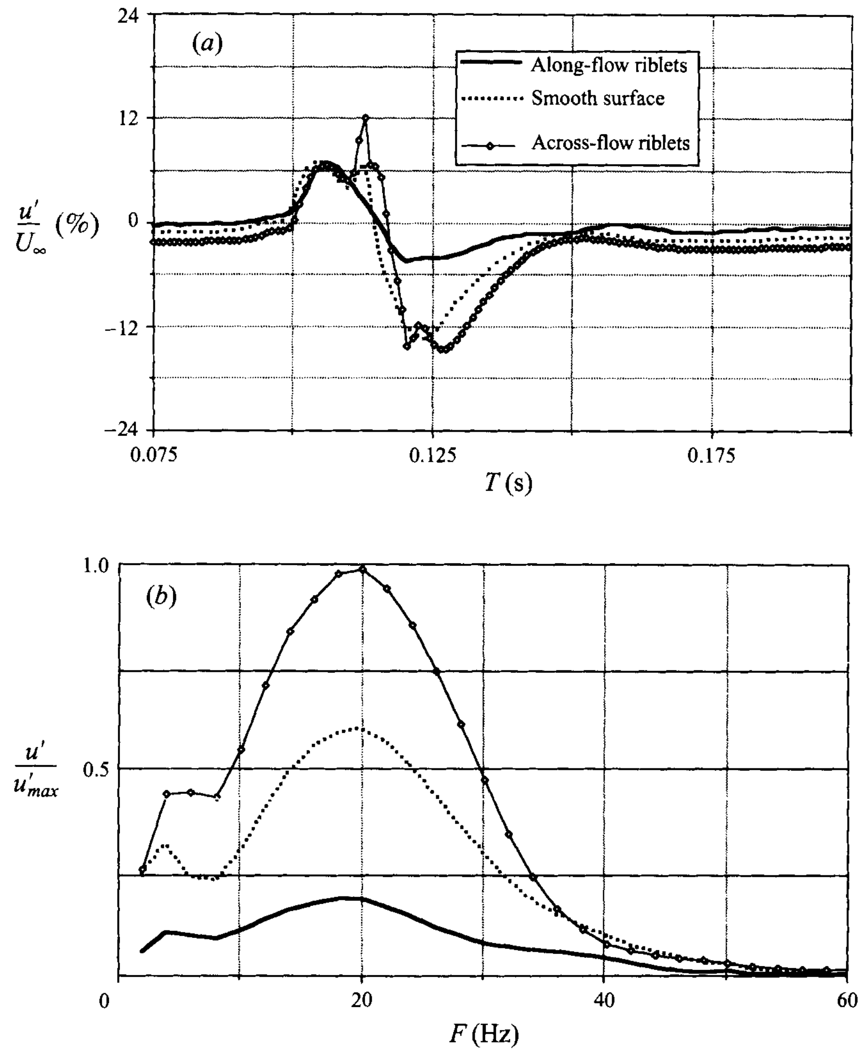

FIGURE 9. (a) Single oscilloscope traces and (b) the corresponding ensemble-averaged spectra measured in the plane of symmetry of the Λ-vortices at $X = 370$ mm, $Y = Y(u'_{max})$, $Z = 0$.

As stated above, the shape and sizes of the riblets were chosen in preliminary experimental investigations. Preliminary study showed the absence of a favourable influence of riblets located flush with the flat-plate surface on Λ-vortex development and hence all measurements were carried out only for riblets located above the flat place surface. This may be connected with the fact that the legs (i.e. a pair of counter-rotating longitudinal vortices) of a Λ-vortex developed on a smooth surface remain insensitive to riblets placed flush with the flat-plate surface further downstream. On the other hand, the linear two-dimensional TS wave senses the influence of these riblets, perhaps, because the maximum of the TS wave amplitude normal to the wall is located almost two times closer to the surface than that of the Λ-vortex. The latter situation results in significant effects of the wall features on the disturbance behaviour.

The influence of the step on the disturbance behaviour is negative probably only for the linear stage of the transition, particularly for TS waves as stated above. However, on the other hand, a small positive influence of the step on localized disturbance (Λ-

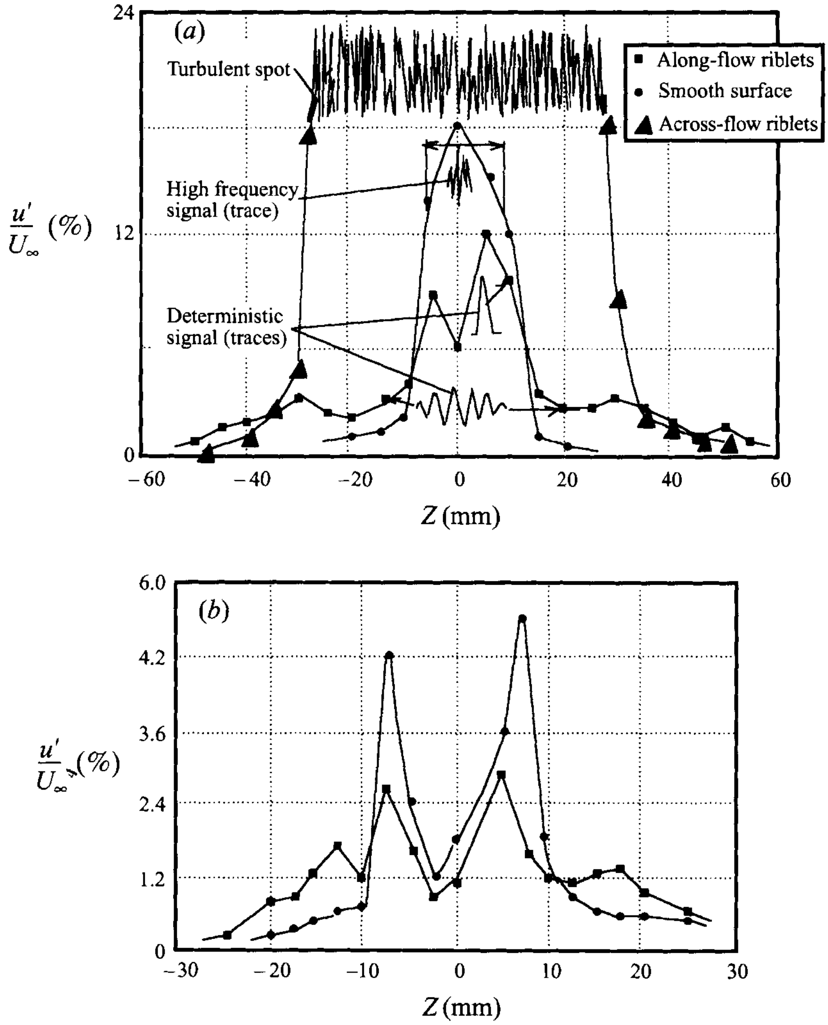

FIGURE 10. The dependence of the disturbance amplitude distribution along the spanwise coordinate (Z) on the longitudinal coordinate (X) for the Λ-vortex development, $Y = Y(u'_{max})$. (*a*) $X = 430$ mm, (*b*) $X = 320$ mm.

vortex-like) behaviour was found in Grek *et al.* (1993). In this case, a smooth plate of 1.2 mm thickness was used instead of a riblet plate. A small reduction in the Λ-vortex intensity was observed, but this influence was almost ten times weaker than the effect of riblets of the same thickness.

3.2.1. *Measurements on riblet plate 1*

The Λ-vortices behaviour measured on the plane of symmetry at $X = 370$ mm on the smooth and riblet surfaces is presented in figure 9. Oscilloscope traces of the disturbance development are shown in figure 9(*a*) and corresponding ensemble-averaged amplitude spectra are shown in figure 9(*b*). The plots show a favourable influence of riblets located along the flow and an unfavourable influence of riblets located across the flow on Λ-vortex development compared to disturbance development on the smooth surface. In the latter case the maximum spectral amplitude of the disturbance is more than two times higher than that of the Λ-vortex development on the riblets; hence the riblets reduce the disturbance intensity both in the maximum of the amplitude spectra and at all frequency bands (see figure 9*b*).

The measurements on the plane of symmetry of the Λ-vortices are very interesting but much more important are the characteristics of the disturbance development along the spanwise direction because the Λ-vortex is three-dimensional. The dependence of disturbance amplitude distributions along the spanwise direction on longitudinal coordinate (X) are shown in figure 10. One can see that distributions at $X = 320$ mm are typical for a Λ-vortex, with two peaks in amplitude located in the region of the Λ-vortex legs and a minimum in amplitude located on the plane of symmetry of this structure. The disturbance intensity on riblets located along the flow becomes less significant than on the smooth surface.

Large changes in the disturbance behaviour take place at $X = 430$ mm. The distribution on the smooth surface has turbulence (high-frequency) fluctuations on the plane of symmetry of the Λ-vortex that indicate a breakdown of the disturbance in this region; on other hand, the distribution on riblets located along the flow remains deterministic in all the measurement area and the distribution on riblets located across the flow showed that disturbances transform into developed turbulent spots. Thus, riblets located along the flow delay the development of the Λ-structure into a turbulent spot, perhaps because the riblets inhibit lateral flow near the surface and thereby act to reduce the removal of low-speed fluid from the wall. This is shown in regions located far from the plane of symmetry, where a strong amplitude gradient for the distribution at the smooth surface indicates increasing vortex activity and a weak amplitude gradient indicates decreasing vortex activity.

3.2.2. *Measurements on riblet plate 2*

The dependence of disturbance amplitude distributions along the spanwise direction on the longitudinal coordinate (X) and on the coordinate normal to the surface (Y) are presented in figure 11. These measurements were carried out on riblet plate 2 ($s^+ =$ 14–17). The riblets in this case were located only above the flat-plate surface and for along-flow riblets. It is seen that distributions at $X = 335$ mm at the smooth and riblet surfaces are almost the same. This is a typical distribution of a Λ-vortex with two amplitude peaks near the structure legs and an amplitude minimum at the plane of symmetry.

Large changes in disturbance behaviour take place at $X = 420$ mm. The distribution at the riblet surface is the usual one for a Λ-vortex, while the distribution at the smooth surface is typical for the beginning of a turbulent spot. This is shown on the inserts in figure 11, where single oscilloscope traces measured in the plane of symmetry (at the stations marked a1, b1) and near the Λ-vortex legs (the stations marked a2, b2) close to surface are shown. Disturbance behaviour on the riblet surface remains deterministic, while disturbances on the smooth surface include the high-frequency fluctuations of the beginning of a turbulent spot. The height of the Λ-vortex above the riblet surface becomes almost one half that above the smooth surface as shown in figure 11.

It should be noted that the behaviour of the disturbances on the smooth and riblet surfaces in regions located far away from the plane of symmetry is similar to the behaviour of the disturbances for riblet plate 1. Namely, the disturbance amplitude distribution over the riblet surface in these regions close to the wall is more rounded and its level is higher than in case of the smooth surface (see figure 11, at $X = 420$ mm, $Y = 1.0$ and 1.5 mm). Both this finding and the reduction of the Λ-vortex height on the riblet surface indicate that possibly the riblets inhibit the movement of low-speed fluid

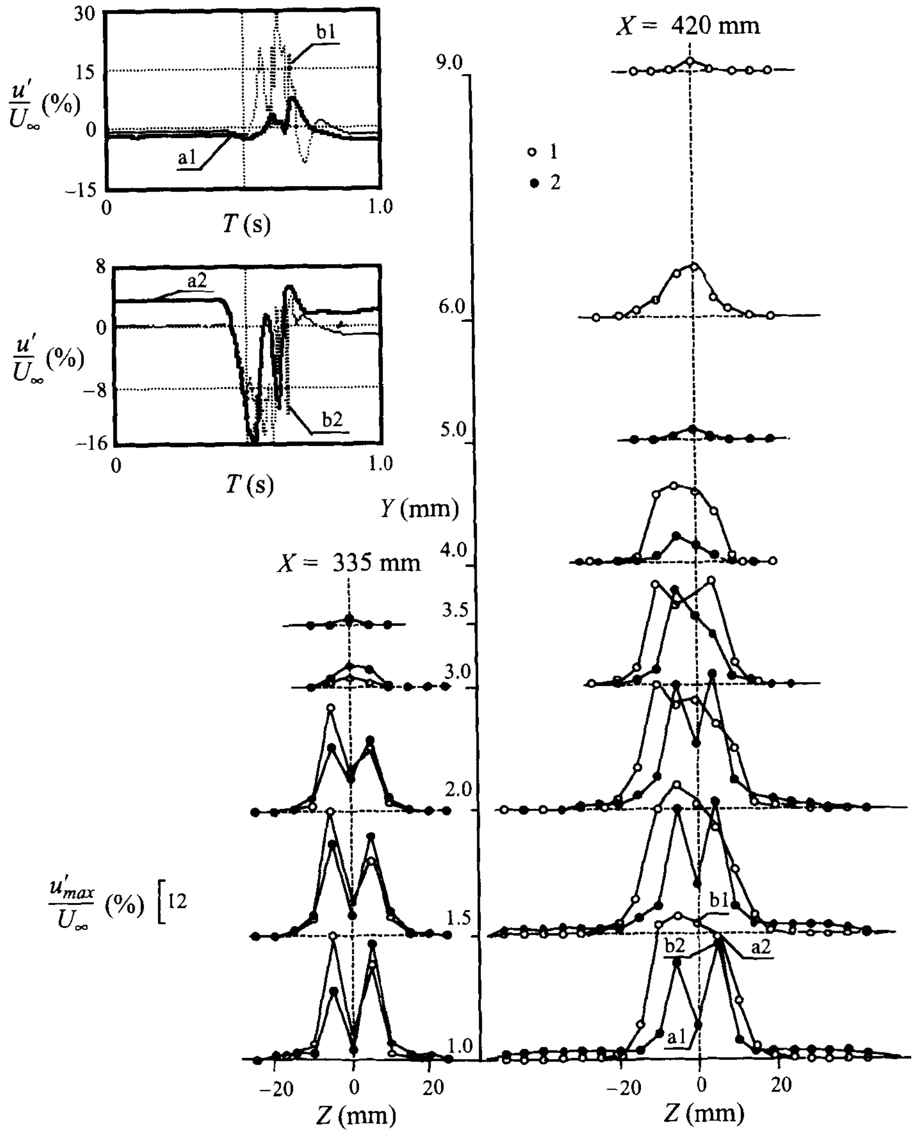

FIGURE 11. The dependence of the disturbances amplitude distribution of a Λ-vortex developed on (1) smooth and (2) riblet surfaces on X, Y, Z coordinates and oscilloscope traces measured at the plane of symmetry (a1, b1) and legs (a2, b2) of the Λ-vortex.

from the surface to the outer region of the boundary layer and hence delay the transformation of the Λ-vortex into a turbulent spot. However, this requires additional study.

Contour diagrams of constant velocity fluctuations ($\Delta u' = \pm 0.05$ m s^{-1}) of Λ-vortex development in the plane of symmetry measured at the smooth and riblet surfaces at $X = 420$ mm are shown in figure 12. One can see the structure of the disturbed flow and the origination of the secondary vortex above the head of the primary vortex for the smooth surface in figure 12(*a*), while at the riblet surface the secondary vortex has not been originated (figure 12*b*).

Spatial–temporal surfaces of constant velocity fluctuation ($u' = \pm 0.05$ m s^{-1}) of Λ-vortex development measured at the smooth and riblet surfaces are shown in figures

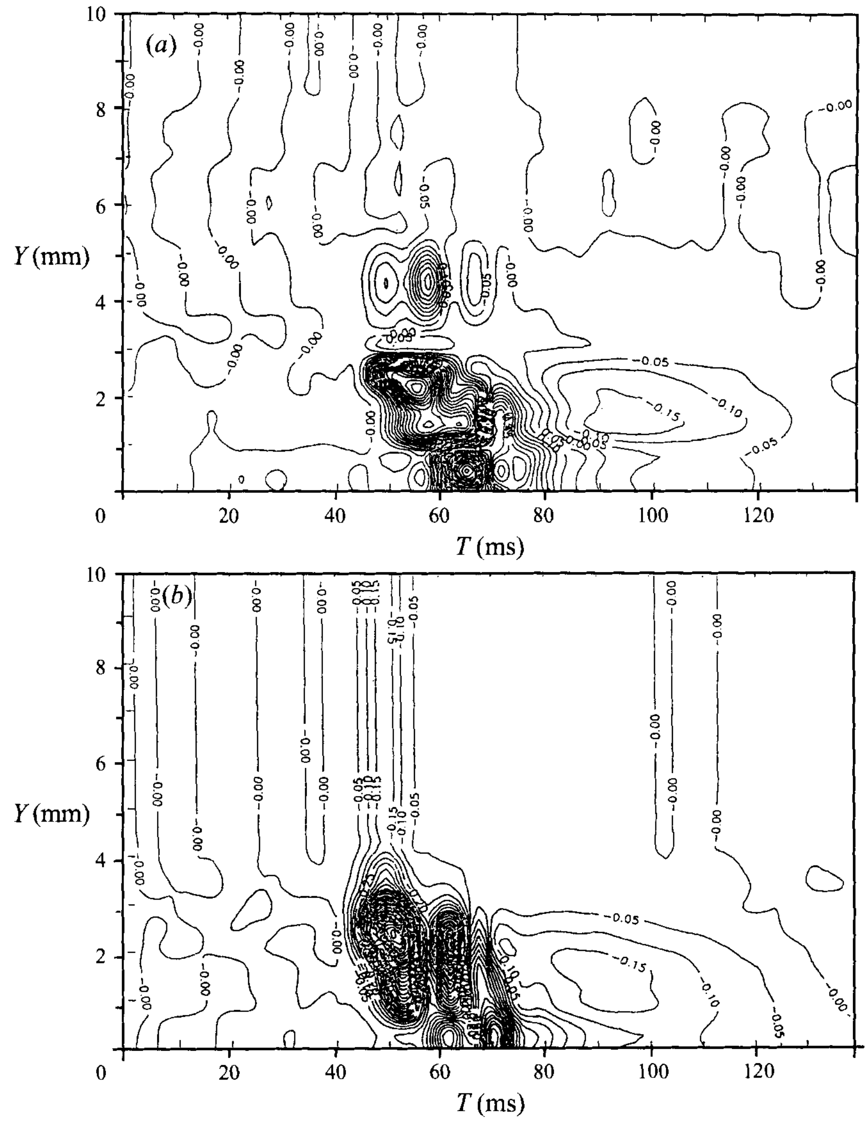

FIGURE 12. Contour diagrams of constant velocity fluctuation for Λ-vortex development measured on its plane of symmetry on (*a*) the smooth and (*b*) riblet surfaces, $X = 420$ mm ($\Delta u' = \pm 0.05$ m s^{-1}), $Z = 0$.

13 and 14. The flow field disturbed by the Λ-vortex at the riblet surface in figure 13 is much less than at the smooth surface in figure 14. On the other hand, the strong peaks of disturbances propagated high over the smooth surface in figure 14 rather disappear in case of the riblet surface in figure 13 and this finding once more demonstrates that riblets reduce the disturbed area of boundary layer flow and hence inhibit transition to turbulence.

3.2.3. *Riblet influence on groups of Λ-vortices*

This experiment was carried out for the so-called K-regime (Klebanoff regime or harmonious regime) of boundary layer transition (see, for example, Saric 1994). A visualization of the K-regime of boundary layer transition is shown in figure 8(*b*) and

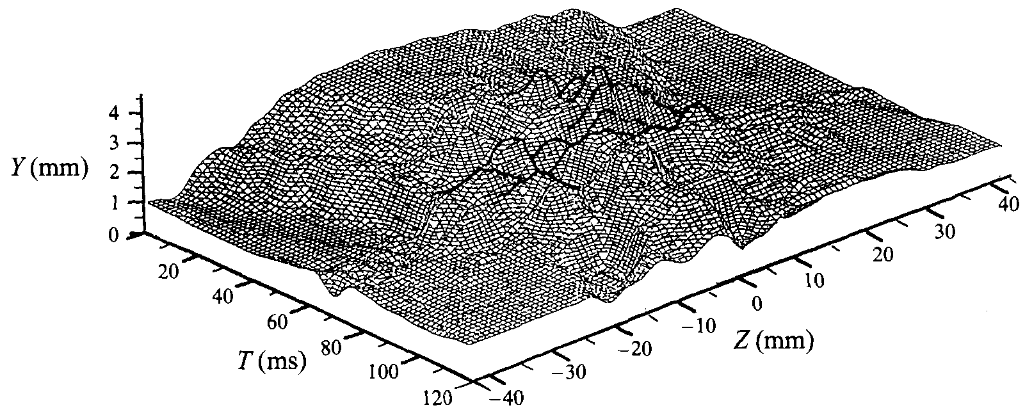

FIGURE 13. Spatial–temporal surface of constant velocity fluctuations ($u' = \pm 0.05$ m s^{-1}) of Λ-vortex development measured on the riblet surface, $X = 420$ mm.

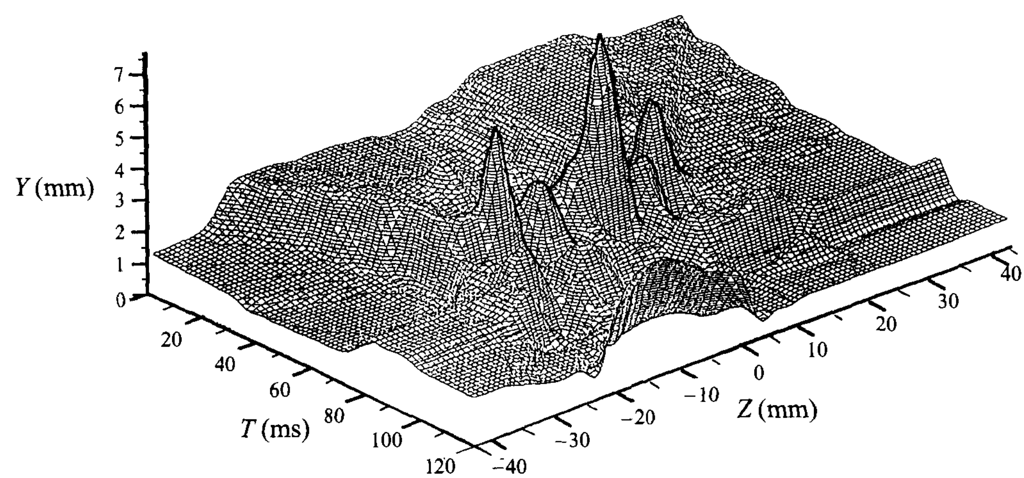

FIGURE 14. Spatial–temporal surface of constant velocity fluctuation ($u' = \pm 0.05$ m s^{-1}) of Λ-vortex development measured on the smooth surface, $X = 420$ mm.

qualitative results of investigations of the development of groups of Λ-vortices for the K-regime of transition at the smooth and riblet surfaces are presented in figure 15. One can see that the influence of riblets on a group of Λ-vortices is the same qualitatively as on a single Λ-vortex but is much stronger.

Thus, riblets with lateral spacing normalized by inner variables ($s^+ = 14$–26) and outer variables (δ^*) ($s/\delta^* = 0.6$–1.3) chosen by preliminary investigations of their influence on the three-dimensional structures (so-called Λ-vortices) were studied to find their effects on both the Λ-vortices and two-dimensional Tollmien–Schlichting waves. Comparison of the influence of the present riblets on the different disturbances of the transition shows that riblets have a positive effect on the localized disturbances of the nonlinear stage of transition and a negative effect on the forced Tollmien–Schlichting waves of the linear stage of transition.

Note, that the optimal non-dimensional drag reduction parameters $s^+ \sim h^+ < 30$ with a maximum drag reduction for $s^+ \sim h^+ = 10$ (see Savill 1989) calculated according

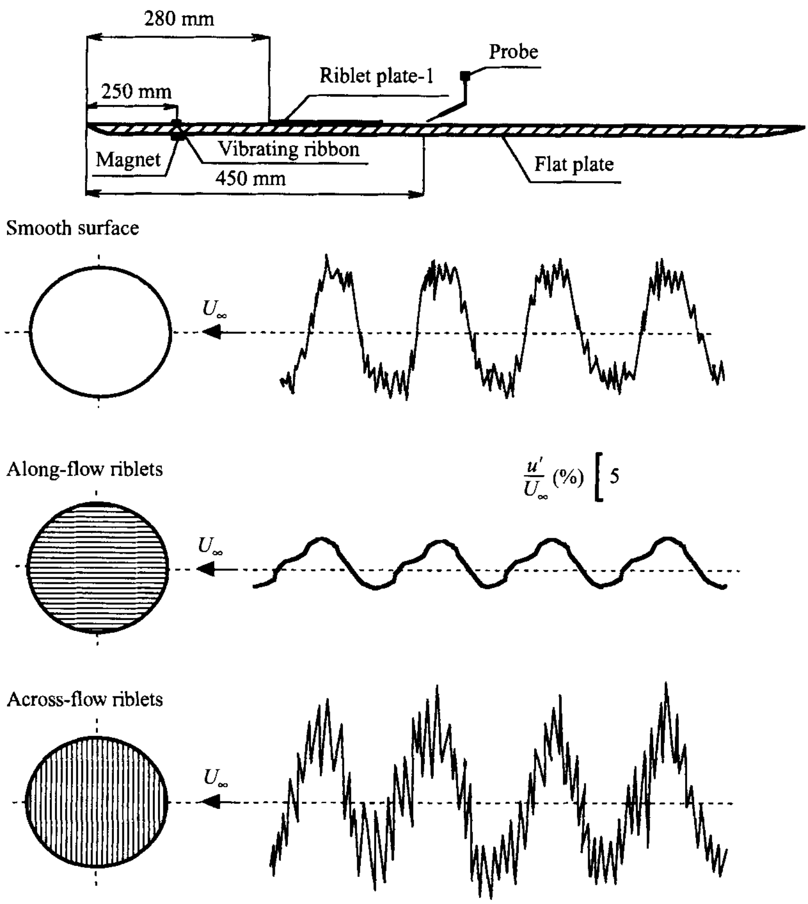

FIGURE 15. Oscilloscope traces of Λ-vortices development on the smooth and riblet surfaces for the K-regime of transition, $Y = Y(u'_{max})$, $Z = 0$.

to inner variables for the viscous sublayer of the turbulent boundary layer are in good agreement with those calculated according to inner variables for the laminar boundary layer in the present case and, on the other hand, it is known that height of the riblets h must not be higher than the viscous sublayer thickness of the turbulent boundary layer. The height of riblets in the laminar boundary layer as shown in the present investigations was approximately equal to one-third of the boundary layer thickness (δ) or displacement thickness (δ^*) $h/\delta^* = 0.5$–1.1.

The riblets ($s^+ \sim h^+ \leqslant 5$, $h/\delta^* \leqslant 0.4$) used by Belov *et al.* (1990) result in acceleration of the transition at $\epsilon = 0.3$ % and the riblets ($s^+ \sim h^+ = 15$, $h/\delta^* \geqslant 0.7$) used by Kozlov *et al.* (1990) result in acceleration or delay of transition at $\epsilon = 1.5$–3 % depending on the experimental conditions (for example, separation flow near the leading edge of the test model led to a shift of the transition point on the riblets further downstream by about 20–50 %). An unfavourable influence of the riblets on the transition in first case is perhaps connected to the effect of the riblets on the TS wave growth rate, while the differences of the riblet influence on the transition observed in second case are due to both bypass transition and experimental situations. Note that the riblet sizes in the latter case are similar to those used in the present investigations.

4. Conclusions

From the results of the present investigations concerning the effects of symmetrical triangular shaped riblets on the behaviour of both two-dimensional Tollmien–Schlichting waves at the linear stage of transition ($s^+ = 22$–26; $s/\delta^* = 1.0$–1.4) and three-dimensional structures (Λ-vortices) of the nonlinear stage of transition ($s^+ = 14$–25; $s/\delta^* = 0.6$–1.3) for flow on a flat-plate the following conclusions can be summarized:

(i) The mean velocity profiles remain unchanged for the bulk of the flow field when the riblets are located along or across the flow and the riblet plate is placed either flush with or above the flat-plate surface.

(ii) Using the riblets for the control of disturbance development at the linear stage leads to growth of the two-dimensional TS wave amplification rates and this process depends strongly on the orientation of the riblets, amplification rates on the riblets located along the flow being much higher than on riblets located across the flow, and their magnitude attains a level of 10% of the free-stream velocity.

(iii) A positive riblet influence on Λ-vortex development was not found when riblets were located flush with the flat-plate surface but was found when riblets were located above the flat-plate surface. It is shown qualitatively that riblet influence on the development of a group of Λ-vortices (the K-regime of transition) is similar to the riblets influence on a single Λ-vortex but stronger.

(iv) Riblets located along the flow delay the transformation of the Λ-vortex into a turbulent spot in comparison with the smooth surface in time and space. Riblets located across the flow accelerate the transformation of the Λ-vortex into a turbulent spot.

These experiments were made possible by the financial support of the Russian Foundation for Fundamental Researches (93-01-17359).

REFERENCES

BACHER, E. V. & SMITH, C. R. 1985 A combined visualization-anemometry study of the turbulent drag reduction mechanisms of triangular micro-groove surface modification. *AIAA Paper* 85-0548.

BECHERT, D. W., BARTENWERFER, M. & HOPPE, G. 1989 The viscous flow on surfaces with longitudinal ribs. *J. Fluid Mech.* **206**, 105–129.

BELOV, I. A., ENUTIN, G. V. & LITVINOV, V. N. 1990 Influence of a flat plate streamwise and spanwise ribbed surface on the laminar-turbulent transition. *Uch. Zap. TsAGI* **17** (5), 107–111 (In Russian). (English transl. in *Fluid Mech. – Sov. Res.*)

BOIKO, A. V., DOVGAL, A. V., KOZLOV, V. V. & SHERBAKOV, V. A. 1990 Instability and receptivity of a boundary layer near the two-dimensional inhomogenous of a surface. *Izv. Sib. Otd. Akad. Nauk SSSR, Ser. Tekh. Nauk* **1**, 50–56 (In Russian). (English transl. in *Sov. J. Appl. Phys.*)

CHOI, K.-S. 1989 Drag reduction mechanisms and near-wall turbulence structure with riblets. In *Structure of Turbulence and Drag Reduction, IUTAM Symp., Zurich* (ed. A. Gyr), pp. 553–560. Springer.

CHU, D., HENDERSON, R. & KARNIADAKIS, G. E. 1992 Parallel spectral-element-Fourier simulation of turbulent flow over riblet-mounted surfaces. *Theor. Comput. Fluid Dyn.* **3**, 219–229.

COUSTOLS, E. & COUSTEIX, J. 1989 Experimental investigations of turbulent boundary layers manipulated with internal devices: riblets. In *IUTAM Symp. Zurich* (ed. A. Gyr), pp. 577–584. Springer.

DINKELACKER, A., NITSCHKE-KOWSKY, P. & REIF, W.-E. 1987 On the possibility of drag reduction with the help of longitudinal ridges in the walls. In *IUTAM Symp, Bangalore* (ed. H. W. Liepmann & R. Narasimha), pp. 109–120, Springer.

DJENIDI, L., ANSELMET, F. G. & FULACHIER, L. 1987 Influence of a riblet wall on boundary layers. In *Turbulent Drag Reduction by Passive Means, Proc. Intl Conf. R. Aeronaut Soc.*, vol. 2, pp. 553–560.

GREK, H. R., KOZLOV, V. V. & RAMASANOV, M. P. 1989 Receptivity and stability of the boundary layer at a high turbulence level. In *Laminar-Turbulent Transition 3, IUTAM Symp. Toulouse* (ed. D. Arnal & R. Michel), pp. 511–522. Springer.

GREK, G. R., KOZLOV, V. V. & TITARENKO, S. V. 1993 Effect of the ribbed surface on a single non-linear wave packet (Λ-vortex) development in a laminar boundary layer. *Sib. Fiz.-Tekh. Zurn.* **2**, 29–36 (In Russian). (English transl. in *Sov. J. Appl. Phys.*)

KOZLOV, V. F., KUZNETSOV, V. R., MINEEV, B. I. & SECUNDOV, A. N. 1990 The influence of free stream turbulence and surface ribbing on the characteristics of a transitional boundary layer. In *Near Wall Turbulence, Proc. 1988 Zorian Zaric Mem. Conf.* (ed. S. J. Kline & N. H. Afgan), pp. 172–189. Hemisphere.

LUCHINI, P. 1993 Effects of riblets upon transition. Abstract submitted to *8th Drag Reduction Meeting, September 23–24, 1993, Lausanne.*

NEUMANN, D. & DINKELACKER, A. 1991 Drag measurements on V-grooved surfaces on a body of revolution in axial flow. *Appl. Sci. Res.* **48**, 105–114.

SARIC, W. C. 1994 Low-speed boundary layer transition experiments. In *Transition: Experiments, Theory & Computations* (ed. T. C. Corke, G. Erlebacherl, M. Y. Hussaini). Oxford University Press.

SAVILL, A. M. 1989 Drag reduction by passive devices – a review of some recent developments. *IUTAM Symp. Zurich* (ed. A. Gyr), pp. 429–465. Springer.

SMITH, C. R., WALKER, J. D., HAIDARY, A. H. & TAYLOR, B. K. 1989 Hairpin vortices in turbulent boundary layers: the implication for reducing surface drag. *IUTAM Symp., Zurich* (ed. A. Gyr), pp. 51–58. Springer.

WALSH, M. S. 1979 Drag characteristics of V-groove and transverse curvature riblets. In *Viscouse Flow and Drag Reduction. Progress in Astronautics and Aeronautics* (ed. G. R. Hough), Vol. 72. Presented at the *AIAA Symp. on Viscouse Drag Reduction, Dallas, Texas, November.*

WALSH, M. S. 1983 Riblets as a viscous drag reduction technique. *AIAA J.* **21**, 485.

WALSH, M. S. & LINDERMAN, A. M. 1984 Optimization and application of riblets for turbulent drag reduction. *AIAA Paper* 84-0347.